Science Advances
AAAS

advances.sciencemag.org/cgi/content/full/5/1/eaau3433/DC1

Supplementary Materials for

Heterogeneous retreat and ice melt of Thwaites Glacier, West Antarctica

P. Milillo*, E. Rignot, P. Rizzoli, B. Scheuchl, J. Mouginot, J. Bueso-Bello, P. Prats-Iraola

*Corresponding author. Email: pietro.milillo@jpl.nasa.gov

Published 30 January 2019, *Sci. Adv.* **5**, eaau3433 (2019)
DOI: 10.1126/sciadv.aau3433

The PDF file includes:

Other Supplementary Material for this manuscript includes the following:

(available at advances.sciencemag.org/cgi/content/full/5/1/eaau3433/DC1)

Table S1. Tidal corrections used with the Lagrangian framework to calculate ice shelf melt rate, derived using the CATS tidal model at the time of passage of the TDX satellites.

TDX DEM acquisition time	CATS 2.0 model tidal prediction (m)
Butterfly	
20110621	-0.45
20120629	-0.34
20130627	-0.41
20140728	-0.28
20160910	0.028
20170627	-0.07
Main Trunk	
20110611	-0.15
20120608	-0.15
20130627	-0.21
20140728	-0.20
20150328	0.57
20160621	-0.05
20170608	-0.06

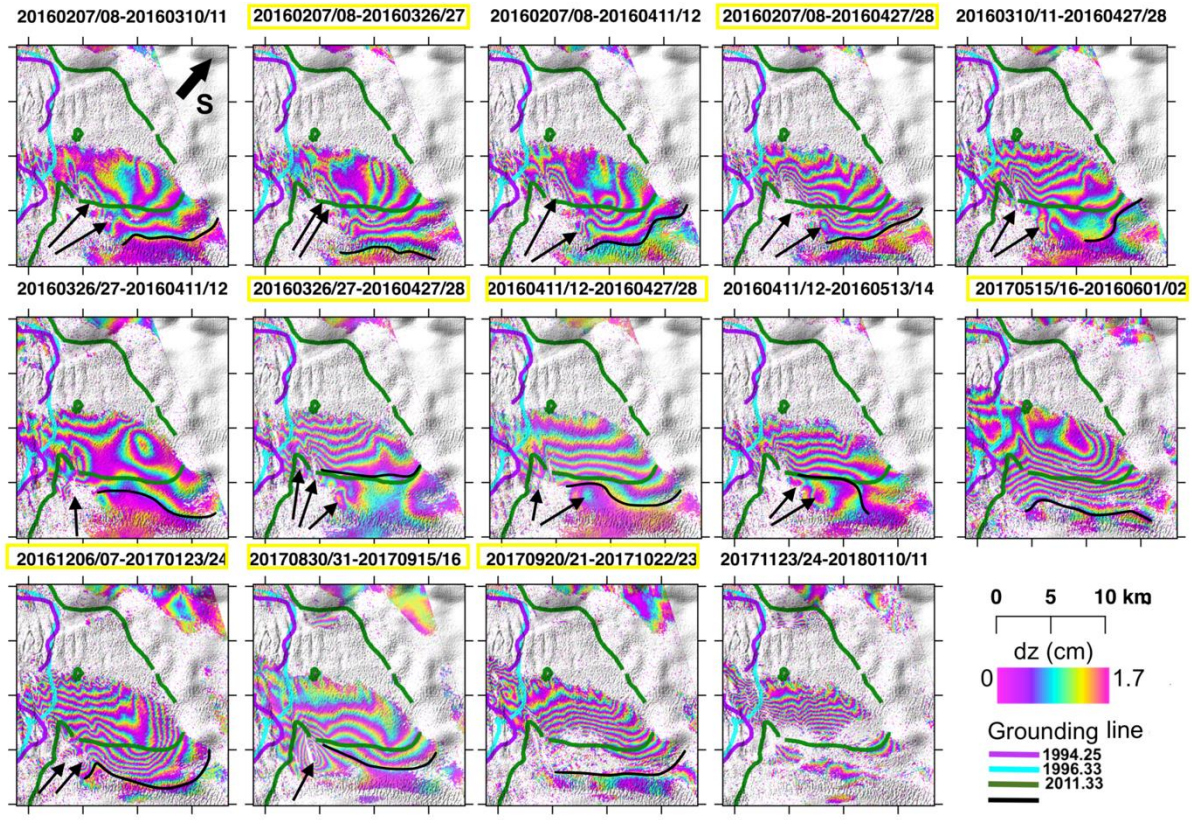

Fig. S1. CSK DInSAR data over the main trunk of Thwaites Glacier. Grounding lines at the acquisition time are shown in black. Older grounding lines used for reference employ purple, blue and green colors. Each fringe, or 360-degree cycle in phase, corresponds to a relative displacement of the ice surface of 1.5 cm in the line of sight of the radar, or 1.7 cm in the vertical direction. Dates are reference image year, month, and day minus slave image year, month and day. Yellow boxes identify DInSAR data with sufficient tidal range to be employed to delineate the grounding zone in Fig. 1. Black arrows identify ephemeral pinning points a few km in diameter within the bending zone. These pinning points disappear with time, indicating vigorous formation of new cavities.

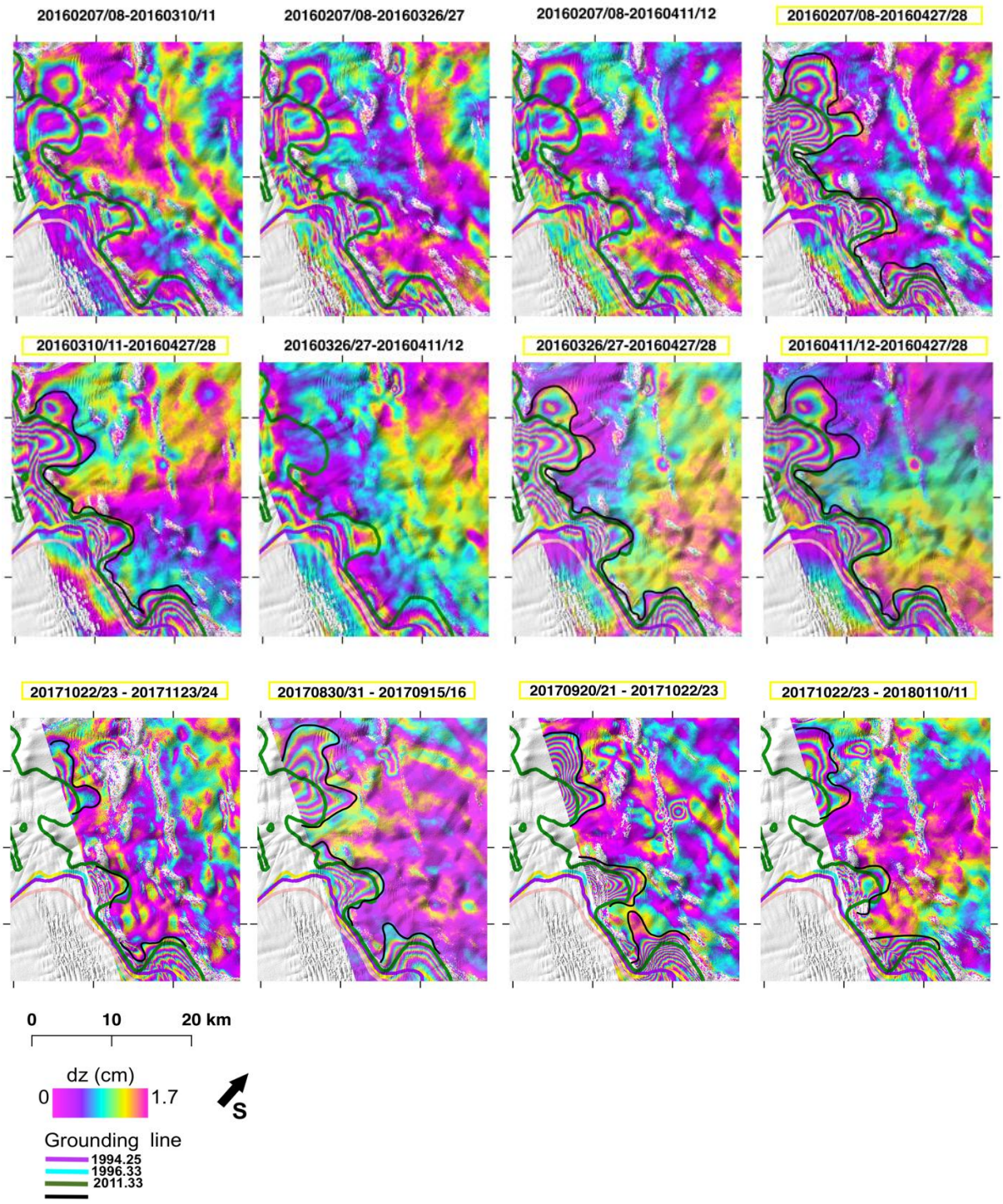

Fig. S2. CSK DInSAR data of the TEIS. West Antarctica from 2016 to 2017. Each fringe, or 360-degree cycle in phase, corresponds to a relative vertical displacement of 1.7 cm. Date convention is similar to fig. S1. Yellow boxes are interferograms used to delineate the grounding zone in Fig. 1. Grounding line positions are color coded for 1994 (purple), 1996 (blue), 2011 (green) and CSK (black).

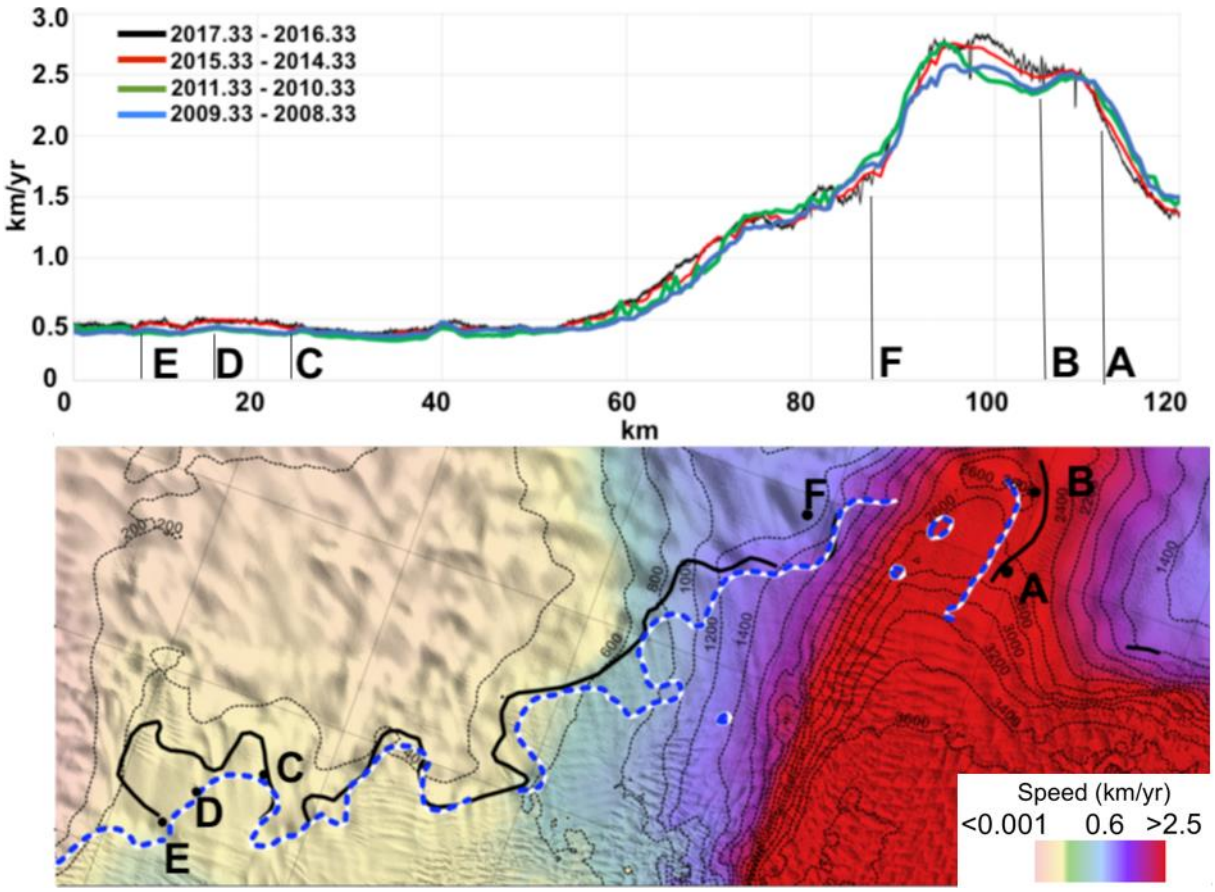

Fig. S3. Speed map over Thwaites Glacier. CSK annual speed (top) in kilometers per year along the year 2011 (blue and white dashed line) grounding line versus the reference velocity (bottom) from year 2016-2017 color coded from brown to red with speed contours every 200 m/yr. Grounding line color coding is the same as in Fig. 1. The results reveal an on-going acceleration in the fast moving, main trunk of the glacier (km 100). CSK average speed is calculated using 14 velocity maps acquired at different tidal heights (fig. S1). CSK standard deviation in speed is 35m/yr. Data from 2009 – 2015 have a standard deviation better than 15 m/yr *(32)*.

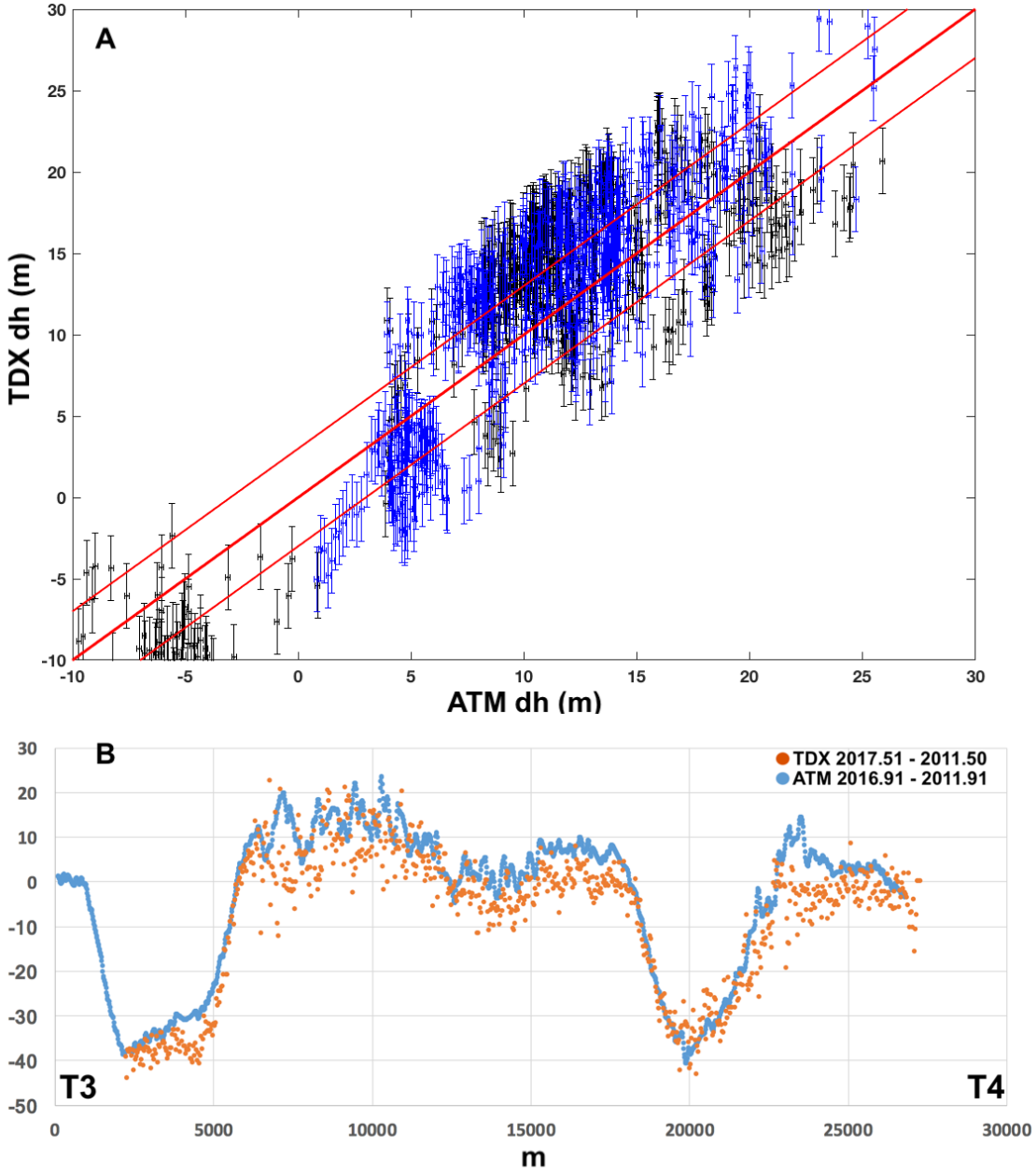

Fig. S4. TDX surface deformation accuracy analysis. (top) Change in ice surface elevation above mean sea level, dh, in meters measured using 2014-2016 ATM data vs TDX over grounded ice for Thwaites Glacier, West Antarctica, along profiles T1-T2 (blue) and T3-T4 (black). The error bar for ATM is 20cm and 2m for TDX. Red lines indicate 1-σ of 4 m. (bottom) Change in surface elevation, dh, in meters measured using the 2014 – 2016/2017 ATM data vs the TDX data over profile T3-T4 in Fig. 3.

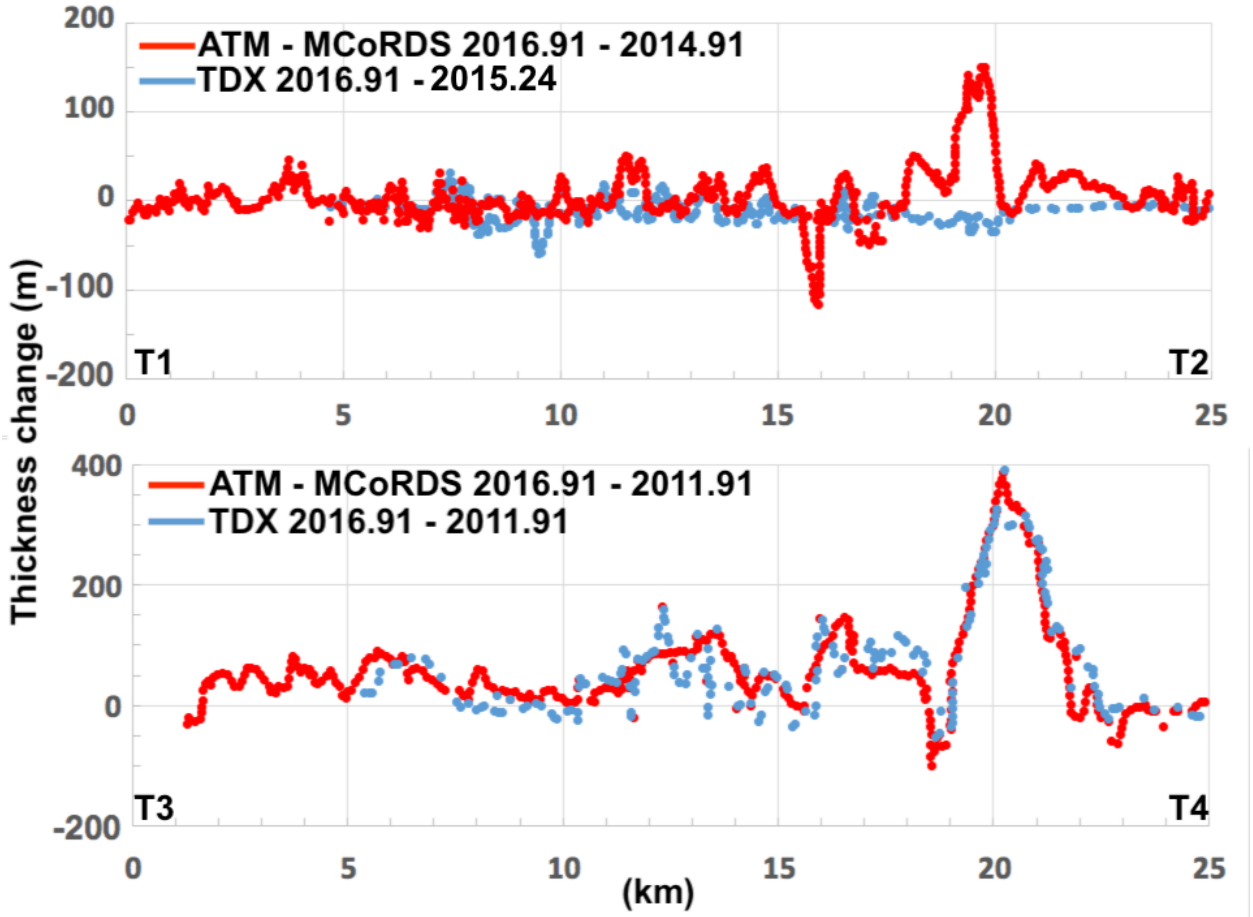

Fig. S5.TDX inferred thickness change accuracy analysis. Thickness change, dH, along profiles T1-T2 and T3-T4 using ATM/MCoRDS (red line) versus TDX (blue line) along profiles T1-T2 (top) and T3-T4 (bottom) in Fig. 3. T1-T2 has data in 2014 and 2016. T3-T4 has data in 2011 and 2016. The agreement is strong for T3-T4 with high melt rates; and weaker for T1-T2 (km 20) with low ice shelf melt rates because hydrostatic rebound of ice biases the TDX results, i.e. the correct value are in red (ATM/MCoRDS). TDX thickness changes are calculated using Eq. 2-3 with a sea surface height of 33.9 m below the WGS84 ellipsoid based on the ATM measurements of ocean surface height.

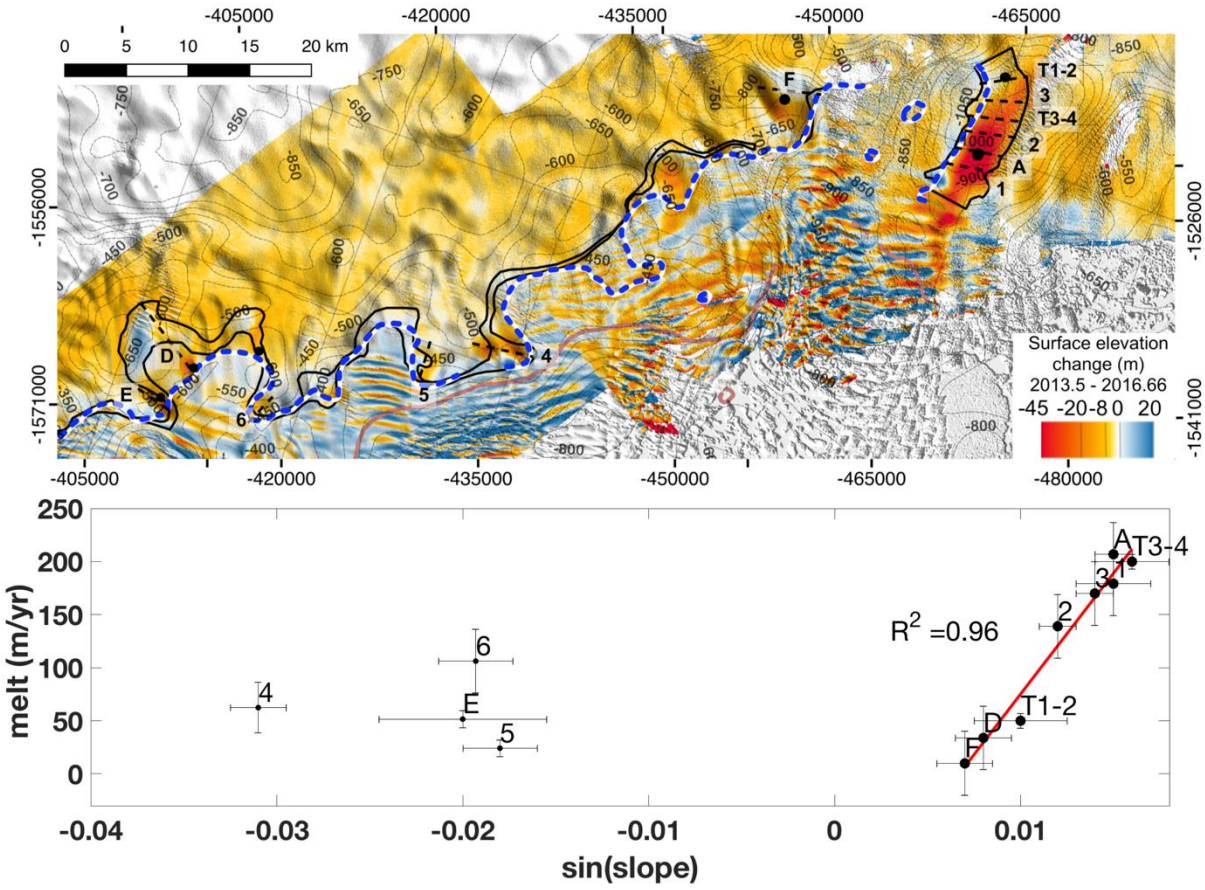

Fig. S6. Relationship between ice shelf melt rate and the ice shelf draft slope. Relationship between inferred ice shelf melt rate (m/yr) and the sine of the slope of the ice shelf draft in the direction of the gradient in melt (dotted line). Ice shelf melt rates include data points from TDX and ATM/MCoRDS. Ice shelf draft slope is calculated using bed topography, which is a proxy for ice draft elevation given that ice is regularly on contact and off contact with the bed across the grounding zone. Positive slopes are prograde slopes, i.e. bed elevation increases in the inland direction. Negative slopes are retrograde slopes, i.e. where bed elevation drops in the inland direction. Locations A-F are shown in Fig. 2. Locations 1-6 are specific to this figure. We note a linear relationship between ice shelf melt and prograde slopes but not for retrograde slopes.

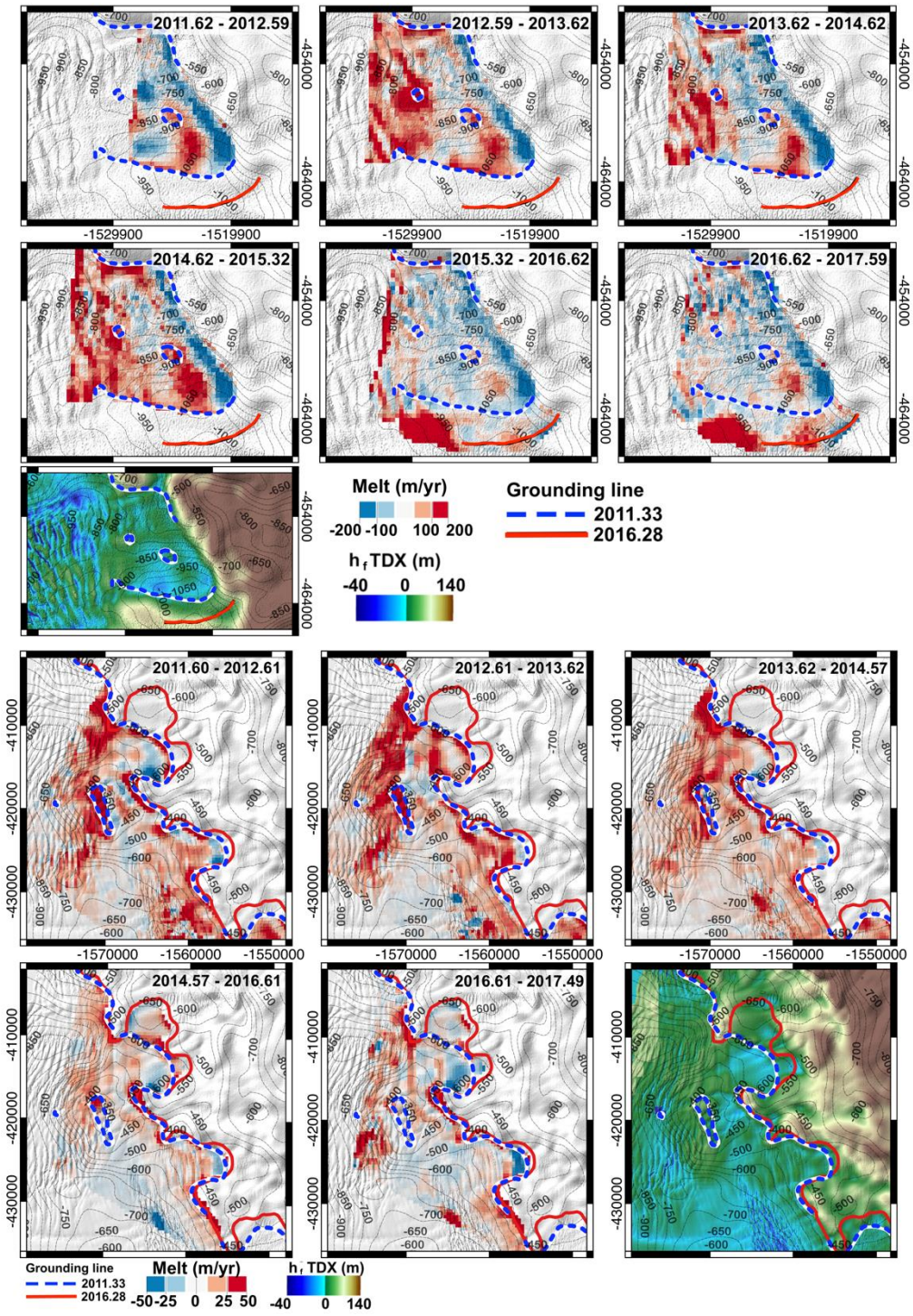

Fig. S7. Annual ice shelf melt rates. Annual ice shelf melt rates in meters per year color coded from -200 m/yr (blue, freezing) to +200 m/yr (high melt) over the floating extension of Thwaites Glacier calculated using a Lagrangian framework, i.e. migrating ice blocks with ice motion and

correcting for flow divergence. (top) Thwaites Eastern Ice Shelf (TEIS) butterfly and (bottom) main trunk of Thwaites Glacier. All TDX elevation data are corrected for tidal height above mean sea level at the time of acquisition of the data (table S1).

Movie S1. TDX time series of surface elevation. Time-series of Tandem-X differences in ice surface elevation, h, overlaid on the bed topography *(16)* with CSK grounding line positions derived from this study (fig. S1).

Movie S2. TDX time series of changes in height above flotation. Time-series of changes in height above flotation, h_f, overlaid on the bed topography *(16)* with CSK grounding line positions derived from this study (fig. S1).